Verification of photon attenuation characteristics for 3D printer based small animal lung model

Se-Ho Lee [a, b], Su Chul Han [b], Seung Wook Lee[a], Seungwoo Park [b*],
[a]*School of Mechanical Engineering, Pusan National Univ., Busandaehak-ro, 63beon-gil 2, Geumjeong-gu, Busan, Republic of Korea*
[b]*Research Center for Radiotherpy , Korea Institute of Radiological & Medical Sciences, 75, Nowon-ro, Nowon-gu, Seoul, Republic of Korea*
[*]*Corresponding author: swpark@kirams.re.kr*

1. Introduction

Small animal such as rodent have been widely used in the clinical and preclinical dose assessment of radiotherapy. Since it is difficult to measure absorbed dose to mice *in vivo*, replica mice are mostly used as alternative. In this study, realistic mouse phantom was fabricated by using 3D printer (object500 connex3, Stratasys, USA). Elemental inks as material of 3D printer were selected corresponding to mouse tissue. To represent lung, selected material was partially used with air layer. In order to verify material equivalent, super-flex bolus was simply compared to verify photon attenuation characteristics. In the case of lung, Hounsfield unit (HU) of the phantom were compared with a live mouse.

2. Methods and Results

2.1 Estimation of photon attenuation characteristics of phantom materials

One of limitations of the 3D printer is that a material of elemental inks are restrict, and besides their linear attenuation coefficients are unknown. Therefore, it is required to estimate photon attenuation property corresponding to mouse tissue. In here, relative photon attenuation characteristics were practically compared with reference material which is super-flex bolus. For comparison, X-ray images of materials within the range of X-ray up to 130kVp were acquired. Since photoelectric absorption process is dominant in low energy X-ray, it is reasonable to compare that range. Figure 1 shows super-flex bolus and selected elemental inks which calls rubber-like. The density of super-flex bolus and rubber-like are $1.03\,\mathrm{g}/cm^3$ and $1.12\,\mathrm{g}/cm^3$, respectively. Thicknesses were fitted to 5mm.

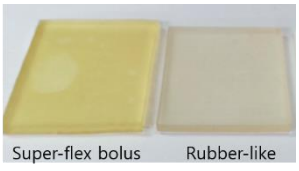

Figure 1. Super-flex bolus and rubber-like

2.2 phantom design

In here, commercial numerical mouse phantom (Moby, Carl E. Ravin Advanced Imaging Laboratories at Duke University Medical Center, USA) was used to get anatomical information. This numerical phantom was converted to digital imaging and communication in medicine (DICOM) format, then the whole body was segmented into bone, tissue, and lung using Mimics software (Mimics, Materialise, Leuven, Belgium). Segmented each image was reconstructed to 3D object, then those object were applied smoothing method by remeshing operation. A smoothing operation factor and iteration value are 0.4, and 5, respectively. The edge mode was selected to perform triangle reduction. These modified objects were converted to stl format which is an input file of 3D printer. Figure 2 shows numerical phantom and mouse phantom fabricated by 3D printer (object500 connex3, Stratasys, USA). The fabricated phantom is a height of 11cm, a width of 3cm, and a thickness of 2.5cm. From an anatomical point of view, fabricated phantom well describe body, bone, and lung. The lung is composed with tissue and air layer, and an abdomen is empty to fill with water for calibration or gel dosimeter for dose assessment. We will deal with verification of lung in the HU analysis.

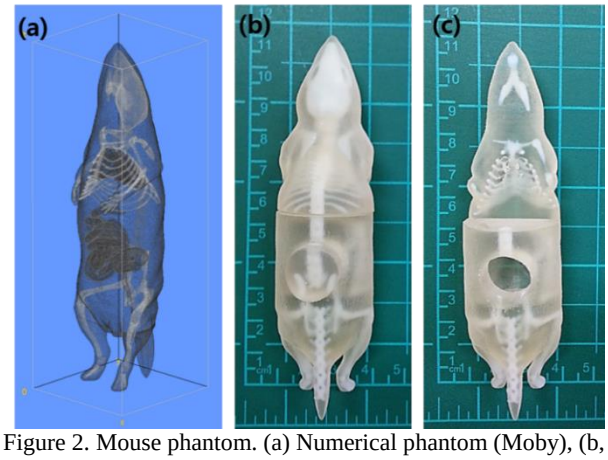

Figure 2. Mouse phantom. (a) Numerical phantom (Moby), (b, c) Mouse phantom fabricated by 3D printer, (b) is whole body, and (c) is inner part showing lung and water tank.

2.3 HU analysis

Computed tomography (CT) images were acquired on a micro-CT system (Pusan National University). Figure 3 shows micro-CT system. An X-ray tube was 70μm focal spot, the number of detector pixel was 2240 x 2344, and a pixel pitch was 50μm. For the scanning, the images were acquired at 55kVp, 300μA, and a distances of SOD (source to object distance) and SDD (source to detector distance) were fitted to 156mm, and 250mm, respectively. A frame rate of detector was 2Hz (0.5msec/frame), and 1 image per 1 degree was acquired. Gantry system was rotated 360 degree, so total 360 images were acquired for scanning.

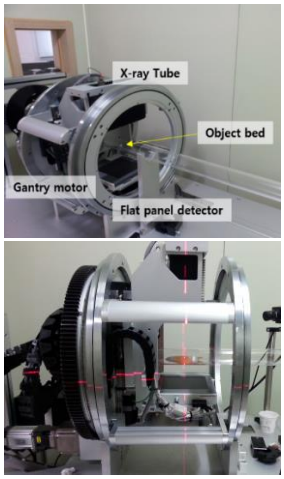

Figure 3. Micro-CT system for tomography scanning

Acquired scanning images were reconstructed to 3D volumetric images by using feld-kamp algorithm, and the reconstructed image was consisted of 512 × 512 × 512 voxels. Figure 4 shows lung images of 3D phantom and live mouse. In order to verify equivalence between them, hounsfield unit (HU) was derivated (eq.1).

$$HU = 1000 \times \frac{\mu - \mu_{water}}{\mu_{water} - \mu_{air}} \quad (1)$$

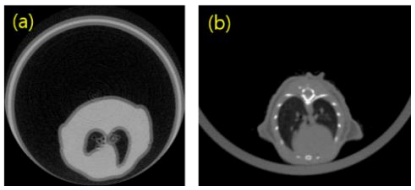

Figure 4. Slice images of lung (a) 3D phantom (b) live mouse

And water phantom was used for calibration. HU values of 3D phantom and live mouse were compared with standard data. Figure 4 shows the results of HU values. In the case of lung, variations between 3D phantom and standard data, and live mouse and standard data are 6.3HU and 40.6HU, respectively. And the tissue shows the variation 17.4HU and 3.2HU. The result shows a variation of 3D phantom and standard data is smaller than live mouse and standard data. Therefore, this study represents that tissue equivalence is valid.

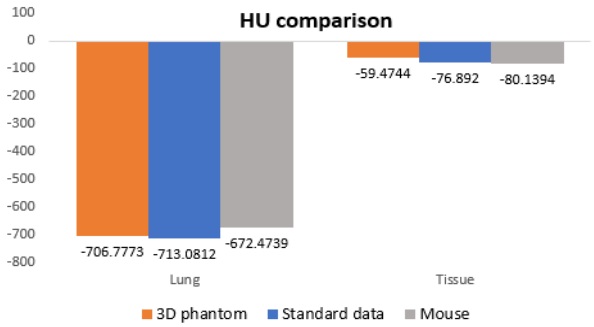

Figure 4. HU comparison of lung and tissue

3. Conclusions

In this study, we fabricated mouse phantom by using 3D printer, and practically verified photon attenuation characteristics. The fabricated phantom shows tissue equivalence as well as similar geometry with live mouse. As more and more growing of 3D printer technique, 3D printer based small preclinical animal phantom would increase reliability of verification of absorbed dose in small animal for preclinical study.

ACKNOWLEDMENTS

This research was supported by Basic Science Research Program through the National Research Foundation of Korea(NRF) funded by the Ministry of Education (No. 2014R1A1A2057004)

REFERENCES

[1] J. Kahn, P. J. Tofilon, and K. Camphausen, Preclinical models in radiation oncology, Radiation oncology, Vol.7, p. 223, 2012.
[2] M. Bazalova, H. Z. Paul, J. Keall, and E. E. Graves, Kilovoltage beam Monte Carlo dose calculations in submillimeter voxels for small animal radiotherapy, Medical physics, Vol.36, p.4991, 2009.
[3] E. Larsson, M. Ljungberg, L. Mårtensson, R. Nilsson, J. Tennvall, S. E. Strand, and B. A. Jönsson, Use of Monte Carlo simulations with a realistic rat phantom for examining the correlation between hematopoietic system response and red marrow absorbed dose in Brown Norway rats undergoing radionuclide therapy with 177 Lu- and 90Y-BR96 mAbs, Medical Physics, Vol.39, p.4434, 2012
[4] Z. Y. Hong, S. H. Eun, K. Park, W. H. Choi, J. I. Lee, E. J. Lee, J. M. Lee, M. D. Story, and J. Cho, Development of a small animal model to simulate clinical stereotactic body radiotherapy-induced central and peripheral lung injuries, Journal of Radiation Research, Vol.55, p.648, 2014
[5] J. Hatton, B. McCurdy, and P. B. Greer, Cone beam computerized tomography: the effect of calibration of the Hounsfield unit number to electron density on dose calculation accuracy for adaptive radiation therapy, Physics in Medicine and Biology, Vol.54, p.N329, 2009